

Project 1 for Complex Adaptive Systems

Vanessa Job

Department of Computer Science
University of New Mexico
vjob@unm.edu

Kellin Rumsey

Department of Mathematics and Statistics
University of New Mexico
knumsey@unm.edu

Abstract—We investigate information flow between higher and lower levels flow of information in models of population growth. We attempt to replicate the results found in [2] and DO OTHER STUFF.

I. INTRODUCTION

Evolution proceeds by emergence of new higher level entities. How information is stored and processed is a driver of this process [2]. For instance, the emergence of epigenetic inheritance provided a competitive advantage through diversification. In this paper, we look at the interaction between organisms as individual populations and organisms considered as a group of populations.

For individual populations, we assume birth rate, death rate, and carrying capacity are all fixed. Define k to be the carrying capacity of a population and n_t to be size of the population at time t . Then the size of the population at generation t is modeled by

$$n_{t+1} = (\text{birthrate} - \text{deathrate})(kn_t - n_t^2)/k \quad (1)$$

If we define the population size relative to the carrying capacity as $x_t = n_t/k$ and define the reproductive fitness $r = \text{birthrate} - \text{deathrate}$, then we get the following equation for x_t :

$$x(t+1) = x_{t+1} = rx_t(1 - x_t), \quad t = 0, 1, 2, \dots \quad (2)$$

This is the logistic map as defined in [3]. In what follows, we will refer to x_t as the population size, with the understanding that it will always be the ratio of the actual population size to the carrying capacity

In [2], the authors investigate information flow between higher and lower levels of organization, between individuals of a population and the population considered as a whole. They study a model that consists of a population of individual populations and examine the direction of the causal information transfer, where "non-trivial collective behavior is associated with the degree to which local elements receive information from the global network." [2]

Their model, a lattice of globally coupled logistic maps, is used to investigate the circumstances under which nontrivial collective behavior occurs. It shows how a reversal in the dominant direction of information flow from bottom-up to top-down is correlated with the emergence of collective behavior of the populations.

FROM INSTRUCTIONS One to two paragraphs that summarize the purpose, methods and analysis of the Walker paper and how you extend that analysis.

KELLIN: State HOW DO WE EXTEND THIS ANALYSIS?

II. METHODS AND RESULTS

A. Sensitive Dependence on Initial Conditions for the Logistic Map

Depending on the value of the reproductive fitness r , the logistic map will generate a population size that is stable, periodic, or chaotic over time. The behavior of the logistic map can vary a great deal with small changes in x_0 . This phenomenon is known as *sensitive dependence on initial conditions*, where small changes in the input lead to large changes in the output. In figure 1, we plot four times series showing population versus time for 50 time steps.

The mutual information measures the dependence of one random variable on another random variable. For two random variables X and Y , we define the mutual information to be

$$I(X, Y) = \sum_{y \in Y} \sum_{x \in X} p(x, y) \frac{\log p(x, y)}{\log p(x) \log p(y)} \quad (3)$$

When two random variables are independent, their mutual information is 0.

We computed the mutual information for the time series in figure 1(a) and figure 1(b). The mutual information for the periodic maps in figure ??(a) is 0.7522 and the mutual information for the chaotic maps it 0.471. This makes sense because after $t = 13$, for the periodic maps, you can certainly determine the value one map by knowing the other. It also makes sense that the mutual information for the chaotic maps should be close to zero because they are chaotic.

To estimate the mutual information, we produced values that could be binned by multiplying each population size by 100 and rounding to the nearest integer. Then we used the JIDT AutoAnalyzer [1] to compute the mutual information assuming discrete data. To generate figure 1 we used Matlab [?] with logistic map equation from [3].

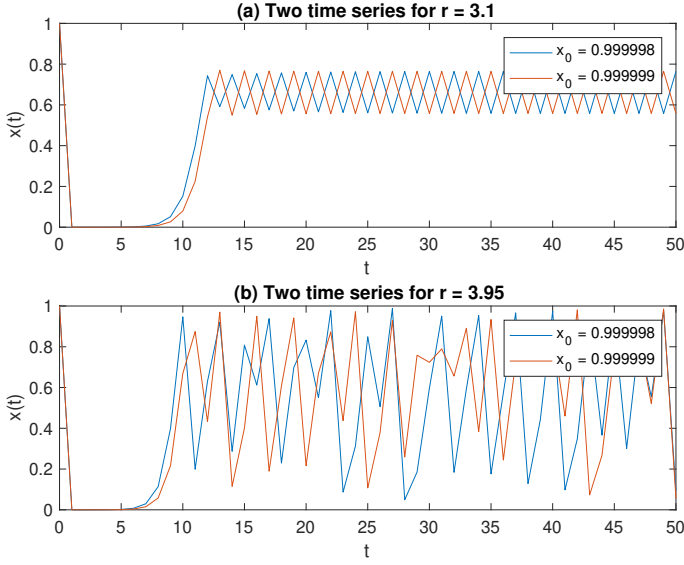


Fig. 1. Population growth over time showing sensitive dependence on initial conditions. The mutual information for the periodic map (a) is 0.7522. The mutual information for the chaotic map (b) is 0.0471.

To test whether binning the data might be adversely affecting our mutual information estimates and since our data was actually real instead of discrete, we also tried IDT's kernel estimator to measure the mutual information. Kernel density estimators are a method for estimating probability densities [?]. The JIDT kernel estimator assumes the input data is Gaussian and approximates distributions for all the variables based on this assumption. One can then use the JIDT AutoAnalyzer to calculate the mutual information between the distributions. Using the kernel estimator, we estimated the mutual information between the periodic maps to be 1.7086 and the mutual information between the chaotic maps to be 0.7192. Again, this validates what we see in 1 because the chaotic maps have less mutual information than the periodic ones.

B. The Walker Model

For this project, we used the model of coupled growth defined in [2]. This model uses a logistic growth model on a lattice of populations coupled with influence from the entire population of populations. For each time step n , the size of population i at time step n is defined to be

$$x_{i,n+1} = (1 - \epsilon)f_i(x_{i,n}) + \epsilon m_n, \quad (i = 1, 2, \dots, N) \quad (4)$$

Here N is the number of time steps, n is the current time step (or generation), and ϵ is the coupling strength of the model to the entire lattice of organisms. Here the local growth dynamics of each population i is defined by

$$f_i(x_{i,n}) = r_i x_{i,n} \left(1 - \frac{x_{i,n}}{K}\right) \quad (5)$$

Here r_i is the reproductive fitness of population i and K is the carrying capacity.

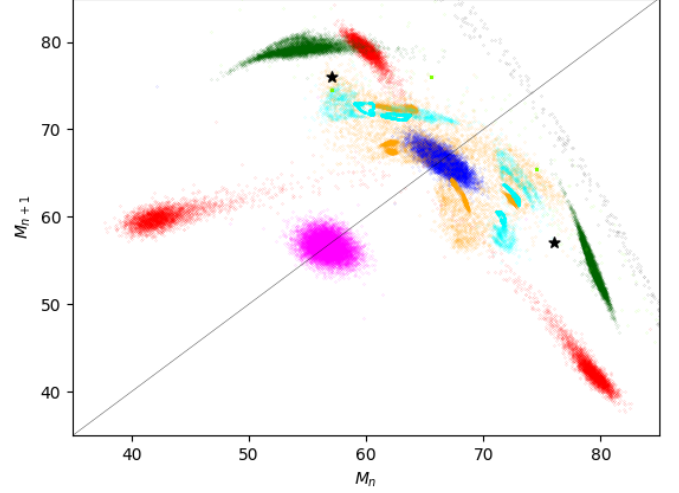


Fig. 2. Return map for selected values of the global coupling strength ϵ : $\epsilon = 0$ (magenta), $\epsilon = 0.075$ (red), $\epsilon = 0.1$ (blue), $\epsilon = 0.25$ (orange), $\epsilon = 0.225$ (aqua), $\epsilon = 0.25$ (dark green), $\epsilon = 3$ (stars) and $\epsilon = 4$ (black)

We model the state of the entire lattice at time n is an average of the states of all the populations. This is called the instantaneous mean field and defined to be

$$M_n = \frac{1}{N} \sum_{j=1}^N x_{j,n} \quad (6)$$

The mean-field m_n is a measure of how the individual populations are growing at any time-step j . It is defined to be

$$m_n = \frac{1}{N} \sum_{j=1}^N f_j(x_{j,n}) \quad (7)$$

The influence of m_i on the entire system is quantified by the parameter ϵ , the coupling strength.

To do our simulation, we set the carrying capacity K to be 100 for all populations i , the number of populations $N = 1000$ and use 10000 time steps. We set the initial population size $x_{i,0}$ to be 1. We also generated a random fitness r_i for each population i .

In figure 2, we show the return maps for a selection of coupling strengths ϵ .

To build the return map, equations 4, 5, 6, and 7 were implemented in Python using Numpy [5] and Matplotlib [6]. The return map shows that when the coupling $\epsilon = 0$, (magenta) there is not much change in how the overall state of the populations changes from time step to time step. That is, populations act as isolated populations. When $\epsilon > 0$, we see a variety of behaviors.

It should be noted that there is quite a bit of dependence on the initial fitness values r_i . In different runs of the return map, $\epsilon = 0.25$ (dark green) and $\epsilon = 0.225$ (aqua) populations sometimes form loops and there can be some scatter instead

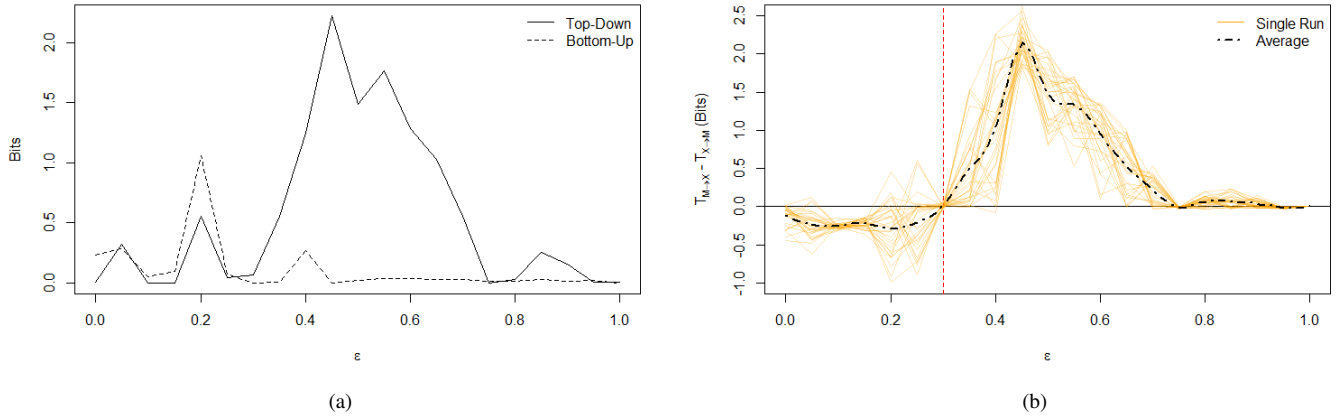


Fig. 3. (a) Top-down, $T_{M \rightarrow X}$ (solid), and bottom-up, $T_{X \rightarrow M}$ (dashed), causal information transfer as a function of the global coupling parameter ϵ for coupled logistic maps. (b) The difference (Top-down minus bottom-up) in causal information transfer for 30 coupled systems as well as the mean as a function of ϵ (dashed). Vertical line at $\epsilon = 0.3$ illustrates the directional reversal of causal information transfer.

of two fixed points when $\epsilon = 0.3$. Overall, we see that coupling strengths 0, 0.075, 0.1 and 0.4 produce predictably shaped regions, while there can be variation in the regions produced by $\epsilon = 0.2$, $\epsilon = 0.225$ and $\epsilon = 0.3$.

While return maps that look like figure 2 seemed to occur more often, it would be interesting to look at the distributions of fitness values r_i that produce the more exotic return maps. This is outside of the scope of this paper.

C. Direction of Information Flow

In order to assess that direction of information flow, from Global to Local scales and vice versa, the authors in [2] take advantage of *Transfer Entropy*. Transfer Entropy is defined mathematically in [8] as

$$T_{Y \rightarrow X}^{(k)} = \sum_n p(x_{n+1}, x_n^{(k)}, y_n^{(k)}) \log \left[\frac{p(x_{n+1} | x_n^{(k)}, y_n^{(k)})}{p(x_{n+1} | x_n^{(k)})} \right]$$

Where $x_n^{(k)}$ is an embedded state in the k -dimensional phase spate defined as $x_n^{(k)} = (x_n, \dots, x_{n-k+1})$.

Although Transfer Entropy is a fine candidate to estimate directionality of this coupling, recent work has focused on improving estimation methods. In their 2015 paper, Gencaga et. al propose new "statistically robust" methodology to estimate Transfer Entropy [10]. Relevant here, is the considerable improvement for continuous processes, where discretizing the data can lead to a distortion in the underlying probability distribution. For this reason, we choose to use the state of the art TransferEntropy package in R and claim based on this work that these estimates of Transfer Entropy are to be preferred.

x

In Figure 3a, we see qualitatively similar results as to what was demonstrated in [2]. The quantitative difference in the location and magnitude of the peaks can be attributed to either chance or estimation method. For low values of the

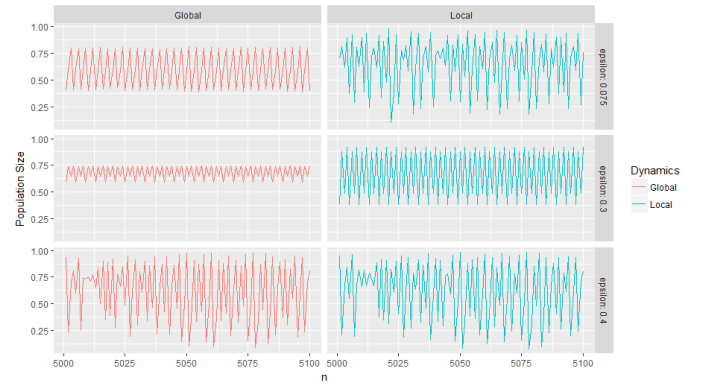


Fig. 4. Population trajectories for an individual (blue) and the mean (red) over 100 time steps. Dynamics are shown for $\epsilon = 0.075$ ($T_{X \rightarrow M} > T_{M \rightarrow X}$), $\epsilon = 0.3$ ($T_{X \rightarrow M} = 0 = T_{M \rightarrow X}$) and $\epsilon = 0.4$ ($T_{X \rightarrow M} < T_{M \rightarrow X}$).

global coupling parameter (ϵ), we see information flow is stronger in the bottom-down direction (from local to global scale). As ϵ increases the direction reverses, and top-down causation begins to dominate. We note again that we are qualitatively in agreement with the previous work [2]. There is however a subtle quantitative difference in our results. It appears from Figure 3a that this reversal of causation occurs at a value of $\epsilon = 0.3$. In an effort to analyze this claim more rigorously, we repeat the entire simulation and estimation procedure 30 times. The right panel of Figure 3 shows the difference $T_{M \rightarrow X} - T_{X \rightarrow M}$ as a function of ϵ for 30 different simulations. The mean is also plotted, and we can see clearly that this reversal of information flow occurs right at $\epsilon = 0.3$. Finally, we note that this result is intuitively satisfactory since it coincides with the black stars in Figure 2, the value of ϵ for which the system is completely synchronized.

D. Additional Analysis

Here we continue our exploration of the relationship between local and global population dynamics. We will use the metric displayed in Figure 3 $T_{M \rightarrow X} - T_{X \rightarrow M}$ to discuss the direction of causal information transfer between the two scales. We break our discussion into 3 cases.

- i) For small values of the global coupling strength, say $\epsilon < 0.3$, Figure 3 shows that our metric takes negative values. This indicates that causal information is flowing from the local to the global scale. The top row of Figure 4 shows that the individual population is chaotic, but the mean trajectory oscillates roughly between 3 values (0.4, 0.6 and 0.6). This is what gives the red points their behavior in Figure 2.
- ii) For $\epsilon \approx 0.3$, the system synchronizes. In fact, we can compute the correlation between the trajectories in the middle row of Figure 4, and see that it is nearly equal to one (0.9879). Based on Figure 2 we should expect these series to oscillate between precisely two values. This particular run had four attractors (black stars) instead of two.
- iii) For large values of the global coupling strength, the global dynamics begin to dominate. There is still a near perfect correlation between M and X , but now even the global dynamics (the mean) behaves chaotically.

For small values of the Global Coupling Strength, say $\epsilon < 0.3$, this metric takes negative values, indicating that information is flowing from the local to the global scale. The top row of Figure ?? shows that the individual populations appear chaotic, but the mean trajectory appears periodic. This is similar to the behavior illus

III. EXTRA CREDIT

Extra credit.

IV. CONTRIBUTIONS

While each of us touched all sections of this paper, Vanessa Job was the primary author of the introduction and the sections about figures 1 and 2, as well as the code that produced the results in these sections. Kellin Rumsey was the primary author of the sections that produced figures 3 and 4, as well as the code that produced the results in these sections.

CHECK THAT BIBITEMS HAVE CORRECT FORMAT

REFERENCES

- [1] Lizier, Joseph T. JIDT: An information-theoretic toolkit for studying the dynamics of complex systems, *Frontiers in Robotics and AI*, 1:11, 2014. [Online] <https://github.com/jlazier/jidt>
- [2] Evolutionary Transitions and Top-Down Causation
- [3] J.M. Mitchell, Complexity. Oxford: Oxford University Press, 2011, pp. 27-37.
- [4] G. Flake, The computational beauty of nature. Cambridge, Mass.:*The MIT Press*, 2011, pp. 139-151.
- [5] Stfan van der Walt, S. Chris Colbert and Gal Varoquaux. The NumPy Array: A Structure for Efficient Numerical Computation, *Computing in Science and Engineering*, 13, 22-30 (2011),
- [6] Hunter, J.D. Matplotlib: A 2D graphics environment. *Computing in Science and Engineering*, Vol. 0, Num. 3, pp 90-95. (2007)[Online] Available: <https://matplotlib.org>
- [7] Moon, Young-Il, Balaji Rajagopalan, and Upmanu Lall. Estimation of mutual information using kernel density estimators. *Physical Review E*, Volume 52, Number 3, September 1995.
- [8] FILL THIS IN
- [9] FILL THIS IN
- [10] FILL THIS IN